NUCL SCI TECH (2018) 29:127
https://doi.org/10.1007/s41365-018-0468-z

Compact lithium-glass neutron beam monitor for SANS at CSNS

Ke Zhou[1,2,3] · Jian-Rong Zhou[2,3] · Yu-Shou Song[1] · Xiao-Juan Zhou[2,3] · Zhao-Yang Xie[1,2,3] · Gui-An Yang[2,3] · Yan-Feng Wang[2,3] · Yuan-Bo Chen[2,3,4] · Zhi-Jia Sun[2,3,4]

Received: 23 October 2017 / Revised: 26 March 2018 / Accepted: 28 March 2018 / Published online: 25 July 2018
© Shanghai Institute of Applied Physics, Chinese Academy of Sciences, Chinese Nuclear Society, Science Press China and Springer Nature Singapore Pte Ltd. 2018

Abstract A small-angle scattering neutron spectrometer for material research is under construction at the China Spallation Neutron Source. An intervening neutron beam monitor behind the sample is needed to measure the beam intensity in order to reduce the measurement uncertainty caused by beam fluctuation. Considering the mobility requirement and limited space, we proposed a compact monitor using a type of lithium-glass scintillator provided by China Building Materials Academy. Its performance was studied experimentally using ^{252}Cf and ^{60}Co sources. The neutron light yield of the selected scintillator was measured to be 5.3×10^3 photons/neutron. The feasibility of *n*-gamma discrimination using the charge comparison method was verified. By using the Geant4 toolkit, the monitor was modeled with precise physical processes including neutron tracking, scintillation, and optical photon transmission. The gamma sensitivity and detection efficiency were investigated in the simulation. It was concluded that a 0.5-mm-thick lithium-glass scintillator with natural lithium is an appropriate choice to satisfy both the neutron detection efficiency and gamma elimination requirements.

Keywords Neutron beam monitor · Lithium glass · *n*-gamma discrimination · Detection efficiency

1 Introduction

We are constructing a small-angle neutron scattering spectrometer (SANS) for material research at the China Spallation Neutron Source (CSNS) [1]. The SANS requires three auxiliary beam monitors in addition to a main detector. Two gas electron multiplier detectors are employed as the beam monitors in front of the scattering sample for their high counting rate ($\sim$ 1 MHz) and excellent spatial resolution [2]. The third beam monitor, behind the sample, is used to suppress the experimental uncertainty due to fluctuation of the neutron beam by counting the neutrons passing through the sample. A ^{3}He counter could be a good option for this function. Considering the international supply of ^{3}He, however, we turn to alternatives to the ^{3}He counter. In recent years, many advanced micropattern gas detectors have been developed for use in neutron beam monitors [3–6]. These detectors can be potential options for use as this beam monitor. However, as an intervening detector, it needs to be repeatedly pulled away from the beam line during neutron

Ke Zhou and Jian-Rong Zhou have contributed equally to this work.

This work was supported by the National Key R&D Program of China (No. 2017YFA0403702), the Instrument Developing Project of the Chinese Academy of Sciences (No. YZ201512), and the National Natural Science Foundation of China (Nos. 11635012, 11405191, and 11205036).

✉ Yu-Shou Song
songyushou80@163.com; yushousong@hrbeu.edu.cn

Zhi-Jia Sun
sunzj@ihep.ac.cn

[1] Fundamental Science on Nuclear Safety and Simulation Technology Laboratory, Harbin Engineering University, Harbin 150001, China

[2] Dongguan Neutron Science Center, Dongguan 523803, China

[3] Institute of High Energy Physics, Chinese Academy of Sciences, Beijing 100049, China

[4] State Key Laboratory of Particle Detection and Electronics, Beijing 100049, China

scattering measurement and plugged in for calibration of transmission neutron counting. Furthermore, limited room is reserved for the monitor in the vacuum of the scattering chamber. It will even be impossible to maintain a gas detector under these conditions. Hence, a design in which a piece of lithium glass equipped with a low-power photomultiplier tube (PMT) is chosen.

Cerium-activated lithium glass has been widely used in nuclear engineering and research as a conventional neutron detector [7–9]. However, we still need to address numerous problems with this particular beam monitoring application. As a neutron beam monitor, it should have a high neutron detection efficiency. However, the beam spot at the SANS is approximately 2.4 cm × 2.4 cm, with a maximum fluence rate of 10^7 n cm^{-2} s^{-1}. The beam intensity is so high that we should balance the detection efficiency and the dead time to guarantee stable operation of the monitor. The uncertainty (statistics) of the measured intensity is expected to be better than 1%. Owing to the high beam intensity, this value will be easy to meet. At the same time, low gamma sensitivity is also required. The disadvantage of using lithium glass as a neutron beam detector is its excessive gamma sensitivity compared with the ^{3}He counter. In current applications, the sensitivity is expected to be below 10^{-4} for gamma rays around 1 MeV. A type of lithium-glass scintillator provided by China Building Materials Academy (CBMA) was studied using the ^{252}Cf neutron source and ^{60}Co gamma source at the Institute of High Energy Physics (IHEP). The charge spectra and neutron light yield were obtained. A neutron beam monitor based on this type of glass scintillator was designed using the Monte Carlo toolkit Geant4 [10].

2 Approaches

The neutron beam monitor is sealed in the vacuum of the scattering chamber, which contains the neutron scattering spectrometer (Fig. 1). This monitor is expected to acquire the beam intensity with high accuracy and appropriate efficiency. It is conventionally designed as an intervening detector. There should be a mechanical module to insert it into and extract it from the beam line. Considering that the dimensions of the monitor must not exceed ϕ80 mm × 150 mm and the monitor should be suitable for moving up and down, we devoted considerable effort to selecting the assembly of the scintillator and PMT. Ultimately, a side-on PMT (e.g., Hamamatsu type R4332) and a low-power high-voltage divider were selected for photoelectric conversion. The lithium-glass scintillator is optically coupled to the cathode window of the PMT by a synthetic quartz light guide. They are placed in a gas-sealed aluminum tube, which is responsible to insulate the outside vacuum and provides a darkroom for the PMT.

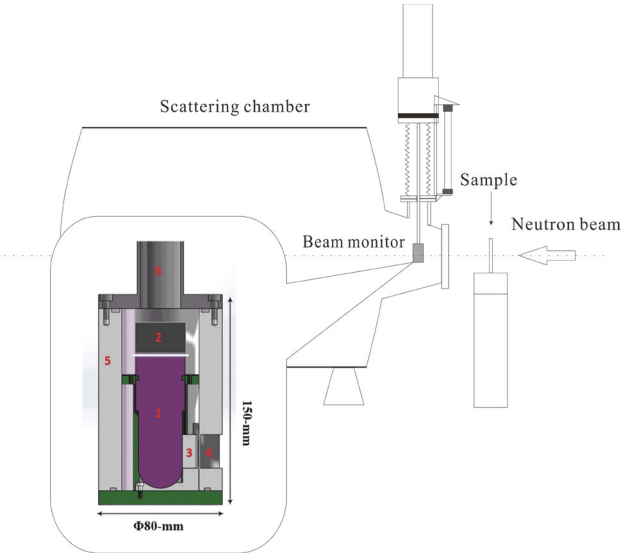

Fig. 1 (Color online) Schematic of SANS terminal at CSNS. In the magnified view of the lithium-glass beam monitor, the parts are tagged as follows. 1. Side-on PMT. 2. High-voltage divider. 3. Synthetic quartz light guide and lithium glass. 4. Neutron incident window. 5. Gas-sealed box. 6. Wire pathway

2.1 Experiment

To investigate the performance of the selected lithium-glass scintillator, an experimental study was carried out. The cylindrical lithium-glass sample has dimensions of ϕ40 mm × 4 mm. It has a total lithium content of 7.7 wt% with ^{6}Li enrichment of 93%. In the experiment, the glass was wrapped in aluminum foil to improve the light collection efficiency. The unwrapped end was mounted on the front window of a PMT (Philips XP2020) by silicone grease. A bias voltage of − 1800 V was applied to the PMT. An oscilloscope (Agilent DSO-X3024A) with an interface developed using LabVIEW was used to perform data acquisition.

The single-photoelectron response of the XP2020 PMT was calibrated in advance. A light-emitting diode with a light wavelength of 395–400 nm, which was chosen according to the maximum scintillation light wavelength of 395 nm, was driven by a pulse generator as the calibration light source. We obtained a single-photoelectron response of 6.2 × 10^2 fC/photoelectron.

The ^{252}Cf neutron source at the IHEP, which has a neutron yield of approximately 1 × 10^6 n/s, was used to study the neutron response of the lithium glass. A diagram of the experimental layout is shown in Fig. 2. The source itself is surrounded by lead sphere shielding to suppress gamma rays. The neutron moderator layer consists of

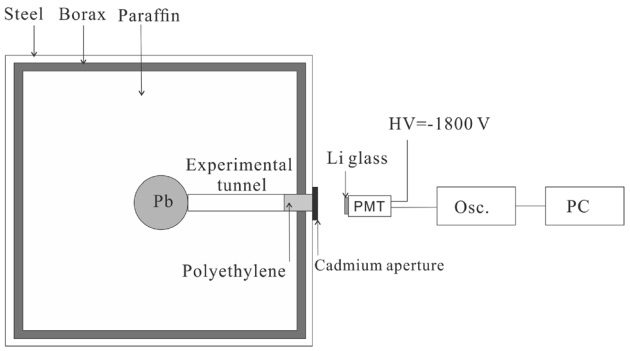

Fig. 2 Diagram of the ^{252}Cf neutron source experiment for studying the performance of the lithium-glass scintillator

35-cm-thick paraffin. A layer of borax with a thickness of 11 cm is placed as the outermost layer for dumping of the moderated neutrons. A neutron beam collimator tunnel with a diameter of 10 cm is prepared starting from the lead sphere and continuing through the neutron moderating and dumping materials. The lithium glass coupled with the PMT is positioned next to the collimator tunnel. Because most neutrons coming through the tunnel are fast neutrons, a cylindrical moderator with a thickness of 10 cm is placed in the tunnel to thermalize the neutrons in this experiment. To study the *n*-gamma discrimination capability of this glass, a ^{60}Co gamma ray source experiment was also carried out using the same experimental setup.

2.2 Monte Carlo simulation

As a traditional choice of neutron beam monitor, the lithium-glass detector has some advantages over the gas detector. (i) It can be processed into a needed shape easily. (ii) The volume is smaller for the same detection efficiency. (iii) No gas-maintaining accessories are required. At the same time, a well-known shortcoming is its excessive sensitivity to gamma rays. Along the neutron beam line of the SANS, the intensity of the associated gamma rays is high. Some of them are direct side products of the neutrons on the spallation target; the others come from neutron reactions with the materials around the spectrometer. To significantly reduce the neutron misidentification due to gamma rays and to establish a proper design, a simulation was performed using the Geant4 Monte Carlo simulation toolkit (version 10.1). The lithium glass that we use is similar to the commercial product GS20; hence, it was modeled with a composition of 18% Li_2O (^{6}Li enriched to 93%), 4% MgO, 18% Al_2O_3, 57% SiO_2, and 3% Ce_2O_3 [11]. All the physical processes related to detection were added within the framework provided by Geant4. The high-precision neutron nuclear reactions model driven by cross-sectional data was implemented to handle the neutron transport. The PENELOPE code embedded in Geant4 was used to simulate the electromagnetic progresses. The scintillation and light collection were modeled using the optical photon package of Geant4 [10]. The attenuation length of the scintillation light is $\sim$ 50 cm [12], which is much larger than the glass thickness. Consequently, the attenuation effect is not significant. The reflectivity of the aluminum foil wrapping was set to 70%. The other scintillating and optical parameters come from reference [13].

3 Results and discussion

3.1 Charge spectra

Typical neutron and gamma-ray signals are displayed in Fig. 3a. The corresponding charge spectra of the lithium glass for ^{60}Co and ^{252}Cf are shown in Fig. 3b. In the spectrum of ^{252}Cf, the left "peak" is attributed to the background on the basis of the experimental result obtained without a source. The right peak is the neutron peak. The light yield of a neutron, *Y*, can be obtained by the following equations:

$$Q_n = Q_s Y \varepsilon_c \bar{\varepsilon}_q, \quad (1)$$

where Q_n is the average charge corresponding to a neutron,

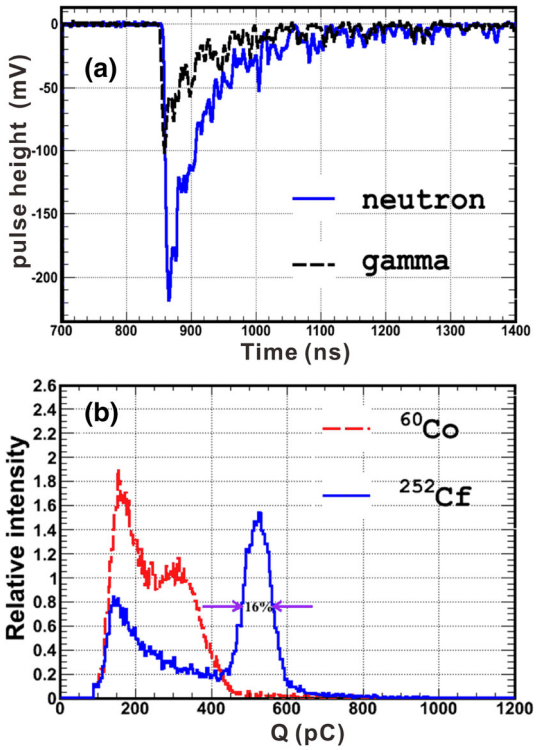

Fig. 3 (Color online) **a** Typical signals of a neutron and a gamma photon, **b** charge spectra of ^{252}Cf neutrons and ^{60}Co gammas

and Q_s is the charge response of a single photoelectron. The charge response of a neutron, Q_n, is 5.3×10^2 pC, which is derived from the peak position of the charge spectrum. The scintillation light collection efficiency, $\varepsilon_c \sim 80\%$, is acquired by a light transition simulation with the Geant4 toolkit, which has been verified in our previous work [13]. $\bar{\varepsilon}_q$ is the average quantum efficiency of the PMT for the scintillation light; it is expressed as

$$\bar{\varepsilon}_q = \int I(\lambda)\varepsilon_q(\lambda)\mathrm{d}\lambda, \tag{2}$$

where $I(\lambda)$ is the normalized scintillation light spectrum, and $\varepsilon_q(\lambda)$ is the quantum efficiency of the PMT for a wavelength λ. We did not measure the scintillation spectrum of this glass. The average quantum efficiency $\bar{\varepsilon}_q$ is approximated by the quantum efficiency $\varepsilon_q \sim 20\%$ at the wavelength of maximum emission (395 nm). Thus, the light yield of this scintillator, Y, for a neutron is determined to be 5.3×10^3 photons/neutron, which is close to that of the commercial lithium glass GS20, 6×10^3 photons/neutron [14].

A thermal neutron is absorbed in lithium glass by the following reaction:

$$n + {}^{6}_{3}\mathrm{Li} \rightarrow {}^{3}_{1}\mathrm{H} + \alpha + 4.78\mathrm{MeV}. \tag{3}$$

The charged ions (the triton and alpha) are emitted with initial kinetic energies of 2.73 and 2.05 MeV, respectively. Their ranges in lithium glass are ~ 40 and $\sim 7\mu$m, respectively, which are far smaller than the thickness of the glass sample. Therefore, the energy deposited by the neutron-produced ions does not generate additional smearing of the neutron spectral peak. The peak width indicates an energy resolution of 16%. In the spectrum of ^{60}Co, the left "peak" comes from the background cut by the threshold. The Compton edges of the two energy lines at 1.173 and 1.332 MeV merge and form a peak-like structure (the right "peak" in the spectrum at $\sim$ 300 pC). Lithium glass is composed of light elements, and the tested sample is thin; therefore, the peak-to-Compton ratio is low. As a result, the photoelectric peaks are merged by the Compton plateau due to the energy resolution. The ^{60}Co spectrum from the Monte Carlo simulation agrees well with that shown in Fig. 3b, where the Compton-edge "peak" position is $\sim$ 0.9 MeV. The neutron peak at $\sim$ 530 pC is distinguished from the gamma spectrum. However, many events overlap each other owing to the gamma sensitivity of the lithium glass. The neutron peak corresponds to an electron-equivalent energy of 1.6 MeV [15]. The positions of the neutron peak and the Compton-edge "peak" together verify the linearity of the PMT gain.

3.2 Gamma sensitivity

Decreasing the thickness of the glass plate is an effective way to reduce the gamma sensitivity of the neutron monitor. The electron-equivalent energy of a thermal neutron $E_{ne} \sim 1.6$ MeVee [15]. An electron with an energy of 1.6 MeV has a range of $\sim$ 2.9 mm in lithium glass. It has a high probability of leaving a glass plate with a thickness smaller than its range before exhausting its kinetic energy. Therefore, the energy deposited by a gamma ray is limited by the thickness of the lithium glass regardless of the energy of a gamma photon. The gamma sensitivity ξ is introduced to evaluate the n-gamma discrimination ability. It represents the probability that a gamma signal with a specific energy is mistaken for a neutron signal. Its value can be derived using the formula [16]

$$\xi = \frac{C_\gamma}{C_t}, \tag{4}$$

where C_γ is the number of gamma rays mistaken for neutron signals, and C_t is the total number of detected gamma rays. According to the experimental result, the energy resolution of the thermal neutron peak given by this type of lithium glass is 16%. A threshold for eliminating gamma events with $E_{ne} - \mathrm{FWHM} = 1.344$ MeV is implemented. Thus, gamma rays depositing energy above the threshold are expected to be mistaken for neutrons.

To validate the code, thermal neutrons and gamma rays with an energy of 1.332 MeV from ^{60}Co are generated to strike a glass scintillator sample 4 mm in thickness in the simulation. The energy spectra are shown in Fig. 4a. They are consistent with the experimental result. When the glass thickness decreases to 2.0 mm, there is no apparent change in the neutron spectrum. However, the neutron–gamma separation becomes larger. Under this condition, even higher energies (e.g., 5 and 10 MeV) lead to a further decrease in the overlap between the neutron spectrum and gamma spectrum. The systematic results for the gamma sensitivity are given in Fig. 4b. When the thickness is 0.5 mm for a gamma energy of 1.5 MeV, the sensitivity of the lithium glass reaches a magnitude of 10^{-6}. This value is close to that of a well-behaved ^{3}He detector with an appropriate threshold [16].

3.3 Lithium glass selection

The width of the pulse output from the lithium glass is 200–300 ns, as shown in Fig. 3a. Accordingly, the counting capability of the monitor based on the lithium glass is approximately $3.3 \times 10^6\ \mathrm{s}^{-1}$ if we ignore the dead time of the electronics. Therefore, the detection efficiency of the

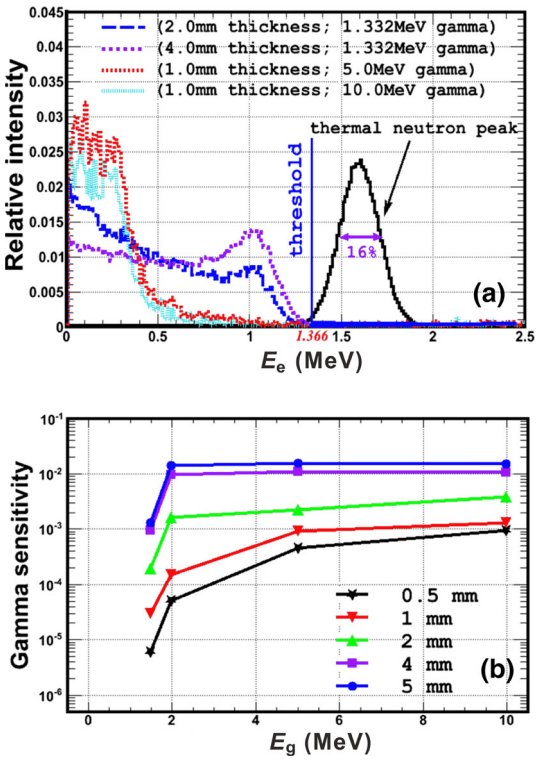

Fig. 4 (Color online) **a** Electron-equivalent energy (E_e) spectra of neutrons and gamma rays given by the simulation, **b** gamma sensitivity of gamma rays with different energy (E_g) in multiple-thickness scintillators

monitor should be kept below 5.7% considering the beam intensity. The simulated neutron absorption efficiency of scintillators with different thicknesses is shown in Fig. 5. The neutron spectrum at the SANS is supposed to peak at the thermal energy (1.8 Å). Thus, we consider a detector design based mainly on thermal neutrons. The thermal neutron absorption efficiency is approximately 59% for 0.5-mm-thick lithium glass. To reduce the scintillator thickness is an effective and direct method to decrease the efficiency. The minimum thickness that the vendor of this type of lithium glass can supply is 0.1 mm. At the same

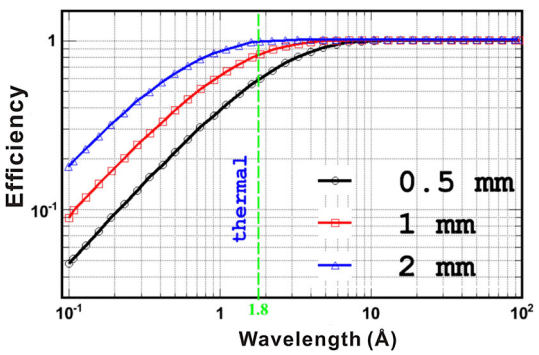

Fig. 5 (Color online) Neutron detection efficiency versus neutron wavelength for different scintillator thicknesses

time, thinner glass also has a lower gamma sensitivity. However, the monitor is supposed to work under a vacuum environment and may be moved frequently into and out of the beam line. When the thickness is less than 0.5 mm, the glass tends to be deformed or even break under the strain caused by the difference in pressure. If defects are created during operation, the measurement accuracy will be affected. Thus, the use of low-enriched or natural (^{6}Li) lithium glass is an appropriate option that yields acceptable gamma sensitivity without mechanical problems. The natural enrichment of ^{6}Li is 7.4%, and that of the glass used in the experiment is 93%. Accordingly, a 0.5-mm-thick lithium glass with natural lithium has a neutron detection efficiency of approximately 4.7%, which satisfies both the gamma sensitivity and efficiency requirements.

4 Summary

The third neutron beam monitor of the SANS at the CSNS must have small dimensions, convenient mobility, and easy maintenance. A monitor design based on a type of lithium glass supplied by CBMA and equipped with a side-window PMT was proposed. The performance of the selected lithium glass scintillator was studied using neutron and gamma sources. A subtle simulation of this monitor based on the Geant4 toolkit was performed. The gamma sensitivity can be suppressed close to the level of a ^{3}He-based detector by decreasing the scintillator thickness. The detection efficiency is sufficiently high even for a piece of 0.5-mm-thick lithium glass. Considering the counting rate capability, we find that a glass scintillator of natural lithium 0.5 mm in thickness is an appropriate selection.

References

1. J. Wei, H.S. Chen, Y.W. Chen et al., China spallation neutron source: design, R&D, and outlook. Nucl. Instrum. Methods A **600**, 10–13 (2009). https://doi.org/10.1016/j.nima.2008.11.017
2. J.R. Zhou, Z.J. Sun, B. Liu et al., Neutron beam monitor based on a boron-coated GEM. Chin. Phys. C **35**, 668–674 (2011). https://doi.org/10.1088/1674-1137/35/7/012
3. G. Croci, G. Claps, R. Caniello et al., GEM-based thermal neutron beam monitors for spallation sources. Nucl. Instrum. Methods A **732**, 217–220 (2013). https://doi.org/10.1016/j.nima.2013.05.111
4. F. Murtas, G. Croci, A. Pietropaolo et al., Triple GEM gas detectors as real time fast neutron beam monitors for spallation neutron sources. J. Instrum. **7**, P07021 (2012). https://doi.org/10.1088/1748-0221/7/07/P07021
5. A. Pietropaolo, R.G. Verona, C. Verona et al., A single-crystal diamond-based thermal neutron beam monitor for instruments at pulsed neutron sources. Nucl. Instrum. Methods A **610**, 677–681 (2009). https://doi.org/10.1016/j.nima.2009.09.013

6. A.C. Stephan, R.G. Cooper, L.F. Miller, Monte Carlo studies of a Micromegas neutron beam monitor. Nucl. Instrum. Methods A **521**, 441–453 (2004). https://doi.org/10.1016/j.nima.2003.09.064
7. Y. Arikawa, K. Yamanoi, T. Nakazato et al., Pr^{3+}-doped fluoro-oxide lithium glass as scintillator for nuclear fusion diagnostics. Rev. Sci. Instrum. **80**, 113504 (2009). https://doi.org/10.1063/1.3254444
8. T. Murata, Y. Arikawa, K. Watanabe et al., Fast-response and low-afterglow cerium-doped lithium 6 fluoro-oxide glass scintillator for laser fusion-originated down-scattered neutron detection. IEEE Trans. Nucl. Sci. **59**, 2256–2259 (2012). https://doi.org/10.1109/TNS.2012.2212458
9. N. Ghal-Eh, R. Koohi-Fayegh, S. Hamidi, Low-energy neutron flux measurement using a resonance absorption filter surrounding a lithium glass scintillator. Radiat. Phys. Chem. **76**, 917–920 (2007). https://doi.org/10.1016/j.radphyschem.2007.01.003
10. J. Allison, K. Amako, J. Apostolakis et al., Recent developments in Geant4. Nucl. Instrum. Methods A **835**, 186–225 (2016). https://doi.org/10.1016/j.nima.2016.06.125
11. G.C. Tyrrell, Phosphors and scintillators in radiation imaging detectors. Nucl. Instrum. Methods A **546**, 180–187 (2005). https://doi.org/10.1016/j.nima.2005.03.103
12. N. Ghal-Eh, M.C. Scott, R. Koohi-Fayegh et al., A photon transport model code for use in scintillation detectors. Nucl. Instrum. Methods A **516**, 116–121 (2004). https://doi.org/10.1016/j.nima.2003.07.058
13. Y.S. Song, J. Conner, X.D. Zhang et al., Monte Carlo simulation of a very high resolution thermal neutron detector composed of glass scintillator microfibers. Appl. Radiat. Isot. **108**, 100–107 (2016). https://doi.org/10.1016/j.apradiso.2015.12.035
14. C.W.E. van Eijk, A. Bessire, P. Dorenbos, Inorganic thermal-neutron scintillators. Nucl. Instrum. Methods A **529**, 260–267 (2004). https://doi.org/10.1016/j.nima.2004.04.163
15. F.W.K. Firk, G.G. Slaughter, R.J. Ginther, An improved Li^6-loaded glass scintillator for neutron detection. Nucl. Instrum. Methods **13**, 313–316 (1961). https://doi.org/10.1016/0029-554X(61)90221-X
16. R.T. Kouzes, J.H. Ely, A.T. Lintereur et al., Neutron detection gamma ray sensitivity criteria. Nucl. Instrum. Methods A **654**, 412–416 (2011). https://doi.org/10.1016/j.nima.2011.07.030